

## **Supplementary Information for "Collective ventilation in honeybee nests"**

Jacob M. Peters,<sup>1</sup> Orit Peleg,<sup>2</sup> and L. Mahadevan<sup>3, a)</sup>

<sup>1)</sup>*Department of Organismic and Evolutionary Biology, Harvard University,  
Cambridge, MA 02138, USA*

<sup>2)</sup>*Paulson School of Engineering and Applied Sciences, Harvard University,  
Cambridge, MA 02138, USA*

<sup>3)</sup>*Department of Organismic and Evolutionary Biology,  
Paulson School of Engineering and Applied Sciences, Department of Physics,  
Harvard University, Cambridge, MA 02138, USA*

---

<sup>a)</sup>Electronic mail: Lmahadev@g.harvard.edu

## A. Supplementary Movies

### 1. *SI Movie 1*

Manual measurements of flow direction, flow speed, air temperature and fanner distribution. This video demonstrates how the data reported in Fig. 1D, Fig. S8, and Fig. S9 were collected.

### 2. *SI Movie 2*

Thermistors suspended in airflow and undisturbed by fanning bees.

### 3. *SI Movie 3*

Manual digitization of fanner position at nest entrance during long-term monitoring.

### 4. *SI Movie 4*

Continuous monitoring of ambient temperature, fanner distribution and temperature profile at nest entrance. This movie is an animation of data reported in Fig. 3C-G.

### 5. *SI Movie 5*

Simulation: Self-organization of fanning groups ( $T_a = 32^\circ\text{C}$ ,  $\Delta T_{max} = 4$ ). This animation tracks fanner density, velocity and temperature during the first 3000 time steps of a simulation in order to highlight the self-organization of a clustered distribution of fanners from an initially uniform distribution. This simulation has the same ambient temperature as those in Fig. 2D-E. Parameters values reported in Table S1.

### 6. *SI Movie 6*

Simulation: Spatio-temporal dynamics of ventilation at  $T_a = 15.5^\circ\text{C}$ ,  $\Delta T_{max} = 20.5$ . This animation complements Fig. 3A1. Parameters values reported in Table S1.

## **7. *SI Movie 7***

Simulation: Spatio-temporal dynamics of ventilation at  $T_a = 30.5^\circ\text{C}$ ,  $\Delta T_{max} = 5.5$ . This animation complements Fig. 3A4. Parameters values reported in Table S1.

## **8. *SI Movie 8***

Simulation: Spatio-temporal dynamics of ventilation at  $T_a = 35.6^\circ\text{C}$ ,  $\Delta T_{max} = 0.5$ . This animation complements Fig. 3A5. Parameters values reported in Table S1.

## B. Study Site

All hives observed were located at Concord Field Station, Harvard University, Bedford, Massachusetts.

## C. Study Organisms

All colonies were originally started from packages derived from Rossman Apiaries in Georgia. The colonies were started with an Italian queen.

## D. Manual measurements

Fig. S1 and Fig. S2 contain the results of manual measurements of fanner distribution, air velocity and temperature at the nest entrance of 4 hives from 07/21/2015 to 07/23/2015. These data complement Fig. 1.

## E. Numerical simulations

The MATLAB code used to generate the data in all figures presented in this paper is available on GITHUB (<https://github.com/jacobmpeters/honeybeeVentilationModel.git>).

### 1. *Parameter choices*

Our simulations tracked the change of local density ( $\rho$ ), local temperature ( $T$ ) and local velocity ( $v$ ) at every position along the nest entrance over each iteration (time). These values were held in three arrays of length  $L/l_b$ .  $L$  was fixed at 38cm, the approximate width of the nest entrance in the experimental setup and  $l_b$  was set to 2cm, the approximate wingspan of a fanning bee. We chose to fix  $T_h$  to 36 °C which is the temperature at which honeybees are known to regulate their core nest temperature<sup>4</sup>. Ambient temperature was fixed throughout each simulation, but was varied across simulations to explore the effects of varying  $\Delta T$ .  $D_v$  and  $D_T$  for Fig. 2 and 3 were  $1 \times 10^{-4}$  and  $4 \times 10^{-5}$ , respectively. These choices were used to fit the simulations to the observed behavior. We explore the effect of these diffusion coefficients on the model's behavior in **Fig. S3**.



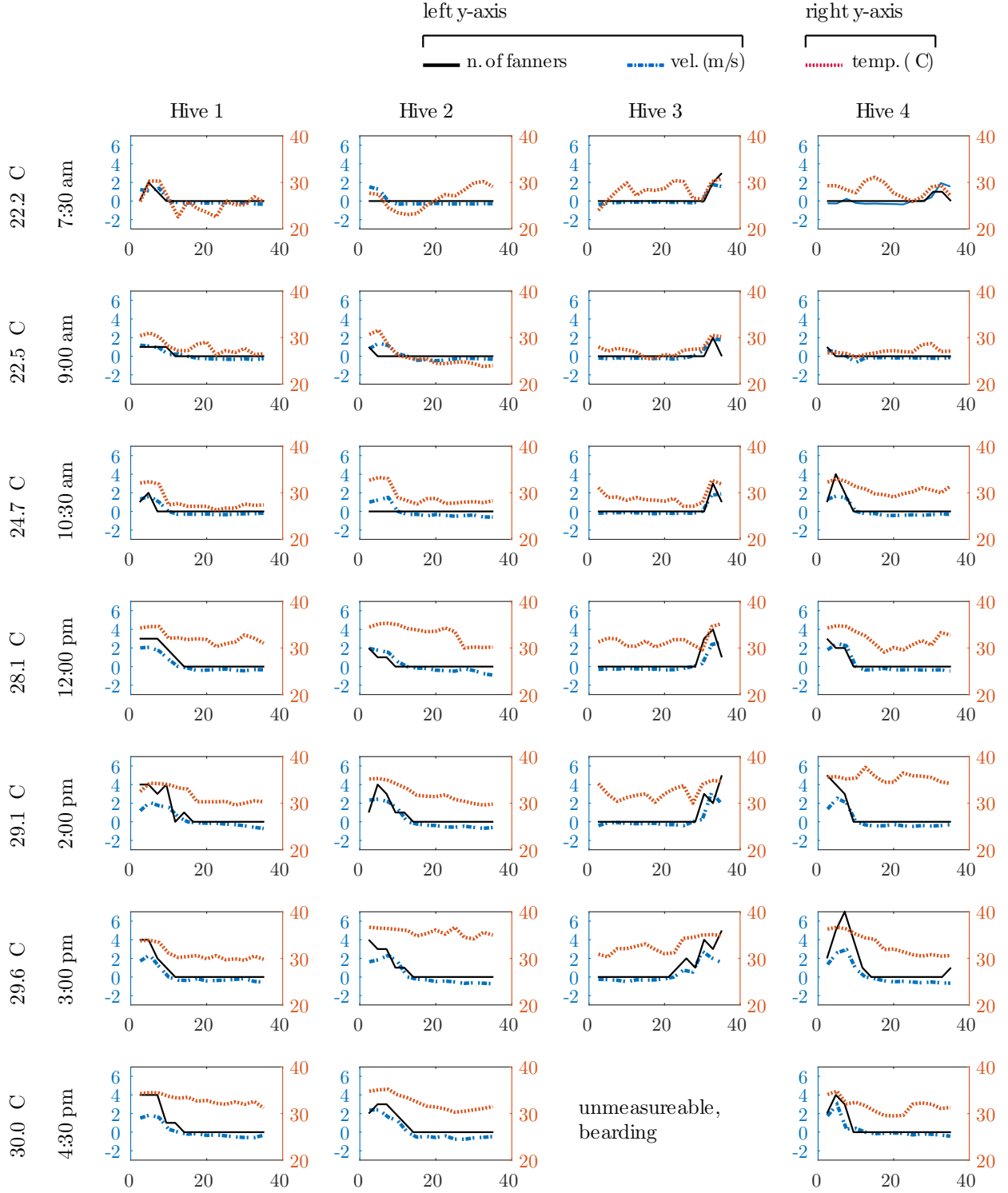


FIG. S1. Fanning activity, air velocity and air temperature as measured along the nest entrance (x-axis, cm). Measurements were made from 4 hives at 7 times throughout the day (07/21/2015). The density of fanning bees, air velocity and air temperature were spatially coupled.

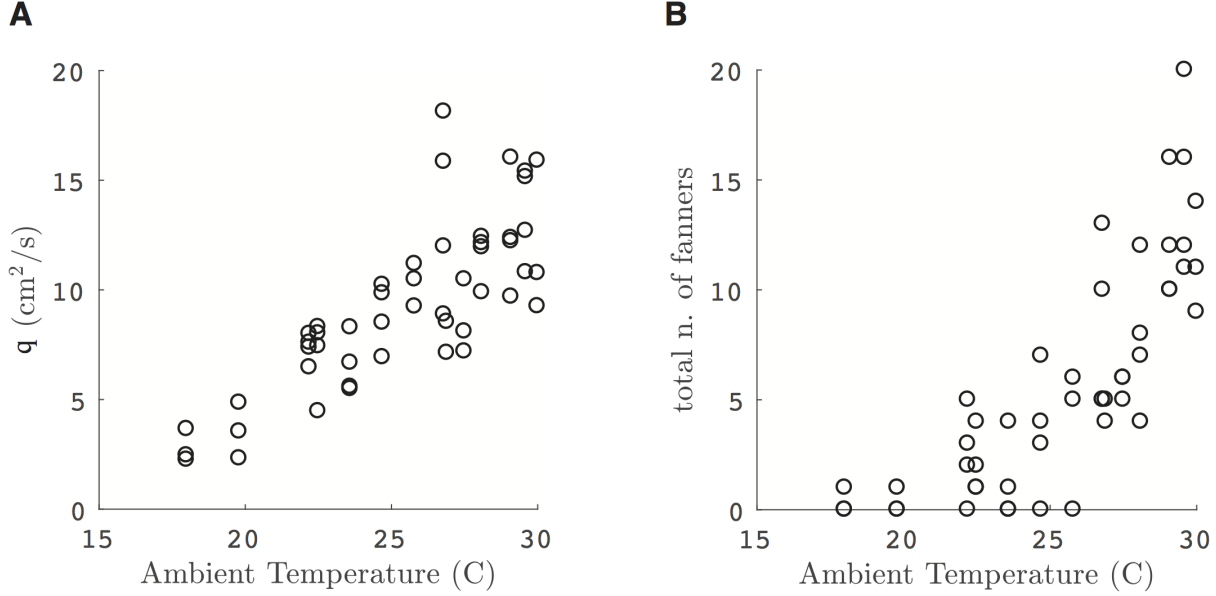


FIG. S2. The relationship between ventilation behavior and ambient temperature according to manual measurements made from 4 colonies from 07/21/2015 to 07/23/2015. (A) Flux of air at the nest entrance ( $q = \frac{\int |v| dx}{2}$ ). Note that because our measurements were sampled from a 1D space, we report flow rate in  $\text{cm}^2/\text{s}$  rather than  $\text{cm}^3/\text{s}$ . (B) Total number of fanners visible at the nest entrance as a function of ambient temperature.

In the continuous form of the model,  $k_{\text{on}}$  and  $k_{\text{off}}$  relate the rate at which bees begin to fan and cease fanning to the local air temperature. In the context of the simulations, these values describe the probability that a bee will fan or cease fanning at a given temperature and are governed by the following equations:  $k_{\text{on}} = k_0 \frac{\tanh(m*(T-36))+1}{2}$  and  $k_{\text{off}} = k_0 - k_{\text{on}}$ . The parameter  $m$  controls the slope of this sinusoidal function. Cook et al. 2013 report the distribution of temperature thresholds above bees will fan when heated in groups of 1, 3 and 10 bees over a range of temperatures<sup>2</sup>. They found that the distribution of temperatures at which individuals are induced to fan is dependent on group size. For the purposes of our study we assumed that the distribution associated with groups of 10 bees was most similar to that which would be found at the hive entrance. We used  $m = 0.1$  because it approximately replicates this distribution. This value also adequately reproduced the same dynamics that we observed at the nest entrance. See SI Fig. S4 to see the effects of  $m$  on ventilation dynamics.

## 2. *Implementation*

We used a finite difference scheme to solve the differential equations. All simulations began with the following initial conditions:  $T$  was set to  $36^\circ\text{C}$  across the entire entrance,  $\rho$  was a uniform distribution (essentially 1 bee per bin), and  $v$  was an array of zeros. At each time step we randomly select one bin of size  $l_b$  and allow  $\rho$  at this bin to evolve according to probability functions  $k_{\text{on}}$  and  $k_{\text{off}}$ .  $\rho$  can change only discretely in multiples of one bee/ $l_b$ . We chose to allow  $\rho$  to change at one position per time step to mimic the discrete decisions made by bees. Equations 2 and 3 were then solved to update the velocity and temperature arrays given the new density array. These steps were then repeated in subsequent loops, each time randomly choosing a position to update.

## 3. *Boundary conditions*

Bees were not allowed to fan at the boundaries, so  $\rho = 0$  at  $x = 1$  at  $x = L/l_b$ . Velocity at the boundaries was also fixed at 0 to enforce the nonslip condition with the walls of the nest entrance. Finally, the diffusion of heat along  $x$  requires a boundary condition that accounts for the thermal conductivity of the boundaries (the walls of the nest entrance), which depends on the thickness and material properties. We implemented a Robin Boundary Condition in which the conductivity of the boundary is controlled by the parameter  $\alpha$ . When  $\alpha \approx 0$ , the wall of the nest entrance behaves as a perfect conductor. When  $\alpha = 1$ , the wall behaves as a perfect insulator. See SI Fig. S5 to see the effect of this parameter choice on ventilation dynamics.

## F. *Mechanisms of self-organization*

Our basic model is derived from the equations of mass and momentum conservation of air flow, recognizing that this flow is driven by bee fanning. We denote the direction parallel to the hive entrance using a coordinate  $x$ , and the direction perpendicular to the hive entrance by  $y$ , the fluid velocity components in the two direction by  $u(x, y, t), v(x, y, t)$  respectively, and the temperature by  $T(x, y, t)$ . Since there are no flows in the  $x$  direction, and no variations in the temperature and flow velocity in the  $y$  direction, we have  $u = 0, v = v(x, t), T = T(x, t)$ . Then, momentum balance in the  $y$  direction reads  $\rho_f(\partial v/\partial t + v\partial v/\partial y) =$

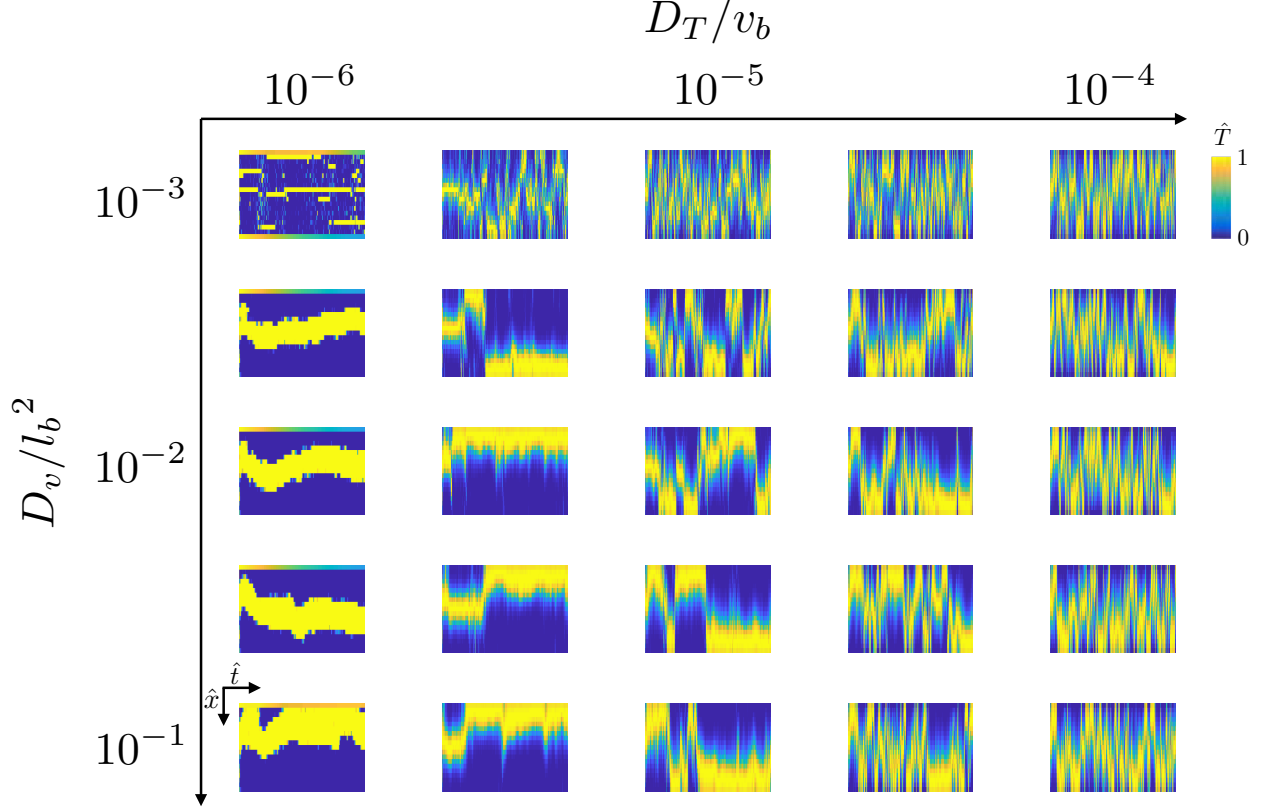


FIG. S3. Effects of diffusion coefficients,  $D_V$  and  $D_T$ , on ventilation dynamics. At low  $D_V$  and  $D_T$ , there is minimal shear imposed by velocity gradients (effective diffusion of velocity) and minimal diffusion of heat through  $x$ . In this condition, the positive feedback between fanning behavior, air velocity and temperature occurs only locally and there is not short-range attraction between fanning groups. This leads to the formation of many small fanning groups. As  $D_V$  and  $D_T$  increase, positive feedback occurs in both space and time. This leads to fewer, larger fanning groups.  $\hat{x} \in [0, 19]$  and  $\hat{t} \in [0, 2 \times 10^4]$ .

$-\partial p/\partial y + f + \mu \partial^2 v/\partial x^2$ , where  $\rho_f$  is the fluid density, and  $f$  is the body force that consists of the fluid friction with the floor of the hive entrance, i.e.  $f = -\zeta v$ , where  $\zeta$  is the friction factor. If the flow reaches steady state relatively quickly compared to any changes in the environment associated with diurnal variations, momentum balance reduces to a simple equation that now reads  $-\zeta v + \mu \partial v/\partial x^2 - \partial p/\partial y = 0$ . Since the pressure gradient is predominantly an active one generated by the bees over their length, a simple expression suggests that  $\partial p/\partial y \sim \rho \rho_f v_b^2$  in the active region where  $\rho$  is the linear density of fanning bees, and  $v_b$  is the constant flow velocity generated by a bee. In the passive region, the pressure gradient is reversed by an amount that is dictated by mass balance. Indeed, integrating the

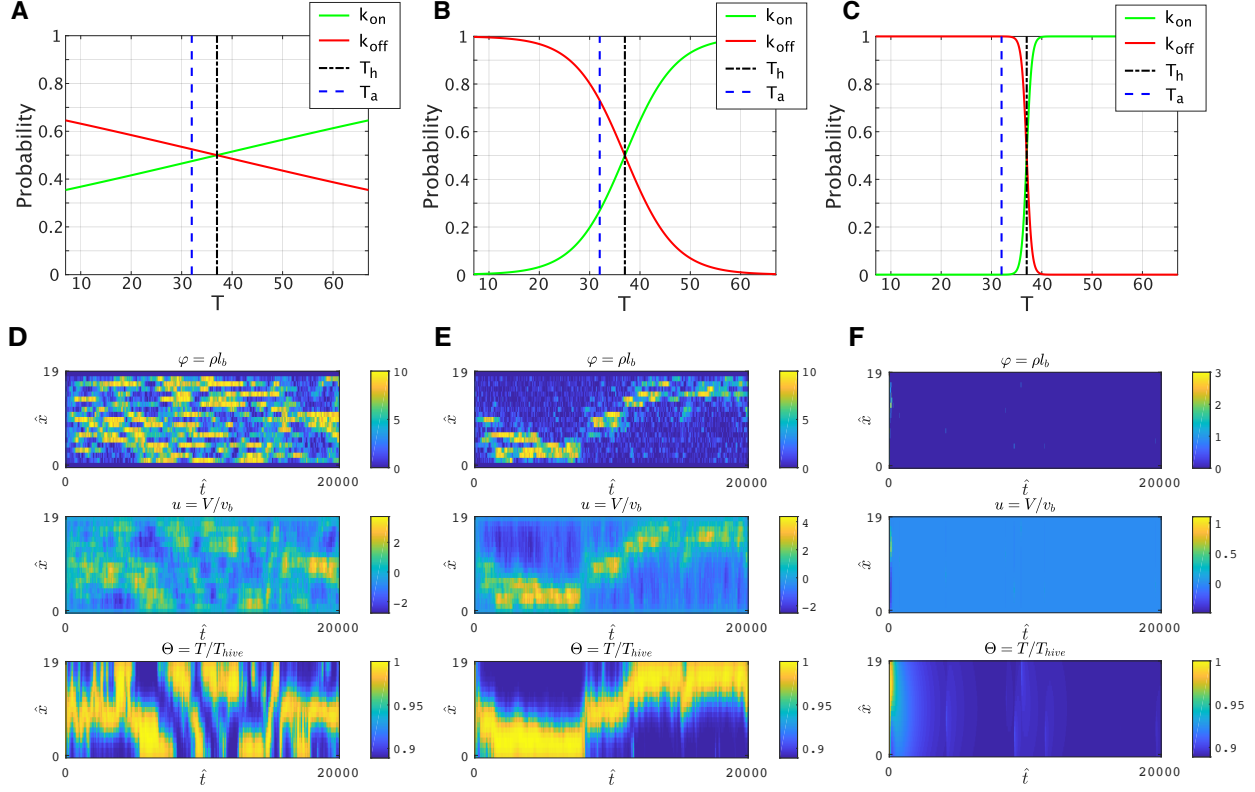


FIG. S4. Effect of slope of behavioral switch functions on ventilation dynamics.  $K_{\text{on}}$  and  $K_{\text{off}}$  prescribe the probability of a given bee to begin fanning or cease fanning at a given local air temperature. The slope of these functions is controlled by the parameter  $m$ . (A,E) When  $m$  is extremely low ( $m = 0.01$ ), fanning behavior is weakly coupled to temperature and no distinct fanning group forms. This leads to high fluid friction and poor ventilation efficiency. (C,E) When  $m$  is extremely high ( $m = 1$ ), fanning behavior will occur only over a narrow range of temperatures. (B,F) At moderate  $m$  ( $m = 0.1$ ), ventilation can occur over a broad range of temperatures and a stable fanning group will form, except when  $T$  is very close to  $T_{\text{hive}}$  ( $\Delta T < 2$ ). Because the slope of these switch functions is the only behavioral parameter in our model—the others pertaining only to the properties of the physical environment—it is likely that natural selection has acted on this parameter to ensure efficient ventilation. We selected  $m = 0.1$  for our simulations because it most adequately fits data on the diversity of fanning temperature thresholds reported in the literature<sup>1,2</sup>.  $\hat{x} \in [0, 19]$  and  $\hat{t} \in [0, 2 \times 10^4]$ .

equation for mass balance over the length of the hive entrance  $L$ , we must have  $\int_0^L v dx = 0$  for global mass balance (assuming that the dominant flow into the hive occurs only at the entrance). Then final equation for fluid flow at the entrance then reads

$$\zeta v = \rho_f v_b^2 \left[ \rho(x, t) - \frac{1}{L} \int_0^L \rho(x, t) dx \right] + \mu \frac{\partial^2 v(x, t)}{\partial x^2}. \quad (\text{S1})$$

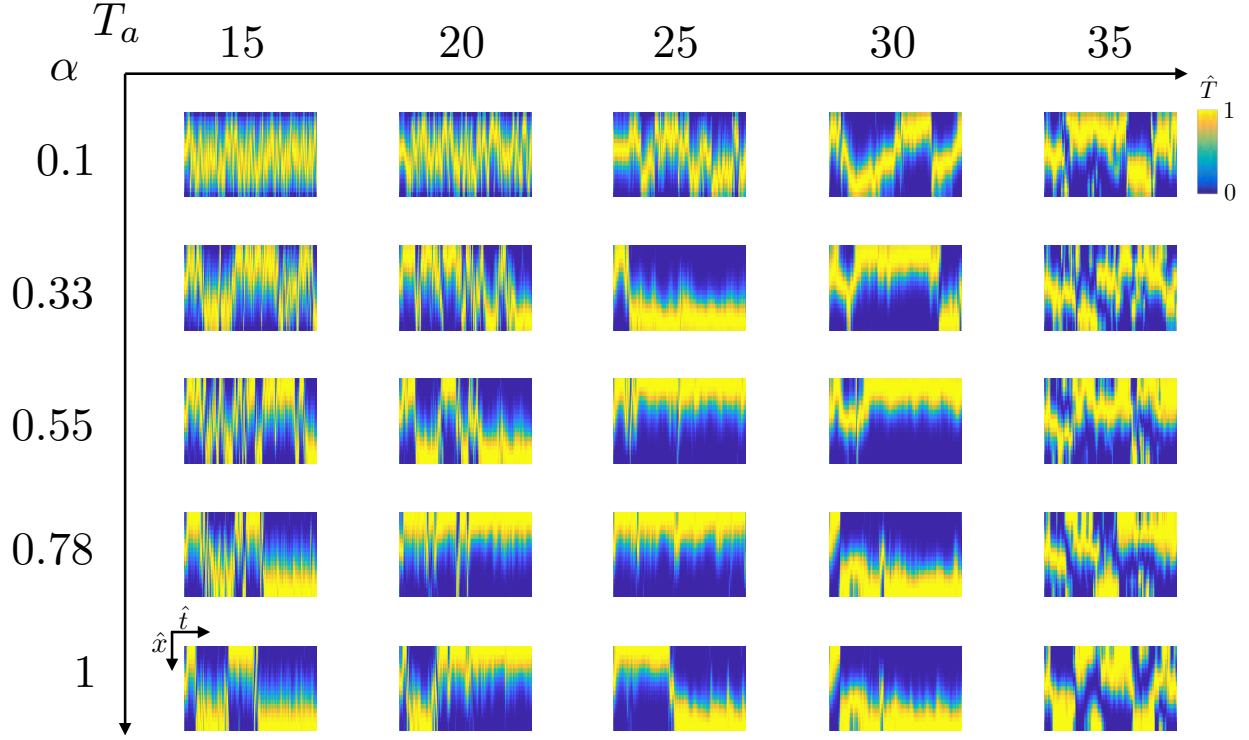


FIG. S5. Effects of ambient temperature and boundary conductivity on ventilation dynamics. The parameter  $\alpha$  controls the thermal conductivity of the boundaries of the nest entrance. When  $\alpha$  is near 0, the boundary is perfectly conductive. When  $\alpha$  is 1, the boundary is a perfect insulator. When  $\alpha$  is small, the fanning group is more likely to occupy the center of the nest entrance. This occurs because heat is being continually lost to the environment through the boundary (if  $T_a < T_h$ ) and the warmest region of the entrance where bees are most likely to fan is the center of the entrance. When  $\alpha$  is high, the system loses no heat through the boundary. Therefore, when the fanning group is positioned at **or** near the boundary, heat diffuses toward the opposite side of the entrance (where inflow is occurring) but not through the boundary. This condition is relatively stable and the fanning bees are more likely to continue fanning near the boundary than they are away from the boundary.  $\hat{x} \in [0, 19]$  and  $\hat{t} \in [0, 2 \times 10^4]$ .

Dividing both sides by  $\zeta$  and defining a characteristic length scale  $l_b = \rho_f v_b / \zeta$  and a scaled momentum diffusivity (with dimensions of the inverse length squared),  $D_v = \mu / \zeta$ , we obtain Eq. (2) in the main text.

For heat balance at the hive entrance, we may write an equation that accounts for advection, diffusion and sources as  $\partial T / \partial t + u \partial T / \partial x + v \partial T / \partial y = D(\partial^2 T / \partial x^2 + \partial^2 T / \partial y^2) + q$ . Again, with the assumptions of variations only in  $x$  and  $u = 0$ , along with a simple cooling law that assumes  $q = -cv\Delta T$ , i.e. the cooling rate is linearly proportional to the temperature difference and the fluid velocity (neglecting any complex dependence on the Nusselt

number), we find that the resulting equation for heat balance at the entrance reads

$$\frac{\partial T(x, t)}{\partial t} = -cv(x, t)\Delta T + D_T \frac{\partial^2 T(x, t)}{\partial x^2} \quad (\text{S2})$$

If we use the dimensionless variables defined by  $\hat{x} = x/l_b$ ,  $\hat{t} = tv_b/l_b$ ,  $u = v/v_b$ ,  $\phi = \rho l_b$ ,  $\Theta = T/T_a$ , we are led to a dimensionless set of our original equations with four dimensionless parameters, given by:

$$u = \left[ \phi - \frac{l_b}{L} \int_0^{L/l_b} \phi d\hat{x} \right] + \frac{D_v}{l_b^2} \frac{\partial^2 u}{\partial \hat{x}^2}. \quad (\text{S3})$$

$$\frac{\partial \Theta}{\partial \hat{t}} = -cl_b u \Delta \Theta + \frac{D_T}{v_b l_b} \frac{\partial^2 \Theta}{\partial \hat{x}^2} \quad (\text{S4})$$

In Fig. S6, we elaborate on the succinct mathematical description indicated in Eqn S1 that describes the dynamics of airflow in and out of the nest entrance. The first term (A) denotes the outward airflow due to the actively fanning bees. However, since the nest volume is fixed, this outflow must be balanced by inflow elsewhere. This simple consequence of fluid conservation demands the presence of the second term (B), which serves as an inhibitor of flow (as it reverses the flow direction). Finally, the last term (C) characterizes the effect of flow entrainment due to the shear induced by motion in and out of the nest; the net effect is that of penalizing large velocity gradients. The accompanying figures show how a population of active fanners leads to a local actively driven outflow, that via conservation of fluid demands passive inflow in those regions where there are no active fanners. The resulting increase in fluid friction due to shear gradients in these regions causes additional entrainment of flow from the nest. This leads to the bees there sensing the nest temperature, driving local recruitment of bees and creating a positive feedback that drives the clusters to coarsen into a single one when the temperature difference between the nest and the environment is large. The different schematics 1,2,3, show how fluid flow can serve as both activator and inhibitor depending on the spatial heterogeneity of the initial density of fanning bees.

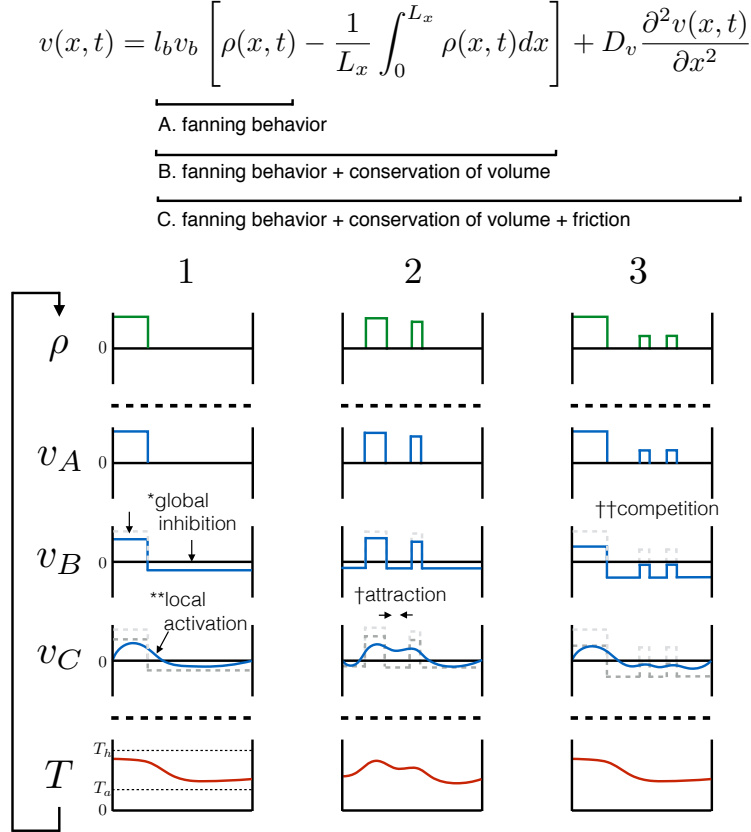


FIG. S6. A schematic illustrating the mechanisms of self-organization which emerge from the model. Equation 2 is broken down into components: (A) the direct result of fanning behavior, (B) conservation of volume, and (C) friction (or effective diffusion of velocity). Below, the following variables are plotted: the distribution of fanners ( $\rho$ ), velocity calculated considering only fanning behavior ( $v_A$ ), velocity calculated considering fanning and conservation ( $v_B$ ), velocity considering fanning, conservation and friction ( $v_C$ ), and the temperature profile ( $T$ ). Scenario 1 is a simple example which illustrates how conservation of volume contributes to global inhibition of fanning behavior (\*) and friction (as well as the diffusion of heat) contribute to local activation (\*\*). That is, bees are more likely to fan adjacent to other fanning bees due to friction and diffusion. Scenario 2 illustrates a case in which this friction/diffusion drives attraction between adjacent fanning groups (†). Fanners are more likely to fan between fanning groups as a result of friction/diffusion. Finally, Scenario 3 illustrates the potential for conservation of volume to act as a global inhibitor which ultimately drives competition between fanning groups (††). Large fanning groups are more likely to grow and smaller groups are likely to shrink and disappear due to this competition.

## G. Long-term hive monitoring

Thermistors were uniformly distributed along the nest entrance ((1.8 x 37cm), leading to a 1.17cm spacing between thermistors. The thermistors were suspended from rigid lead



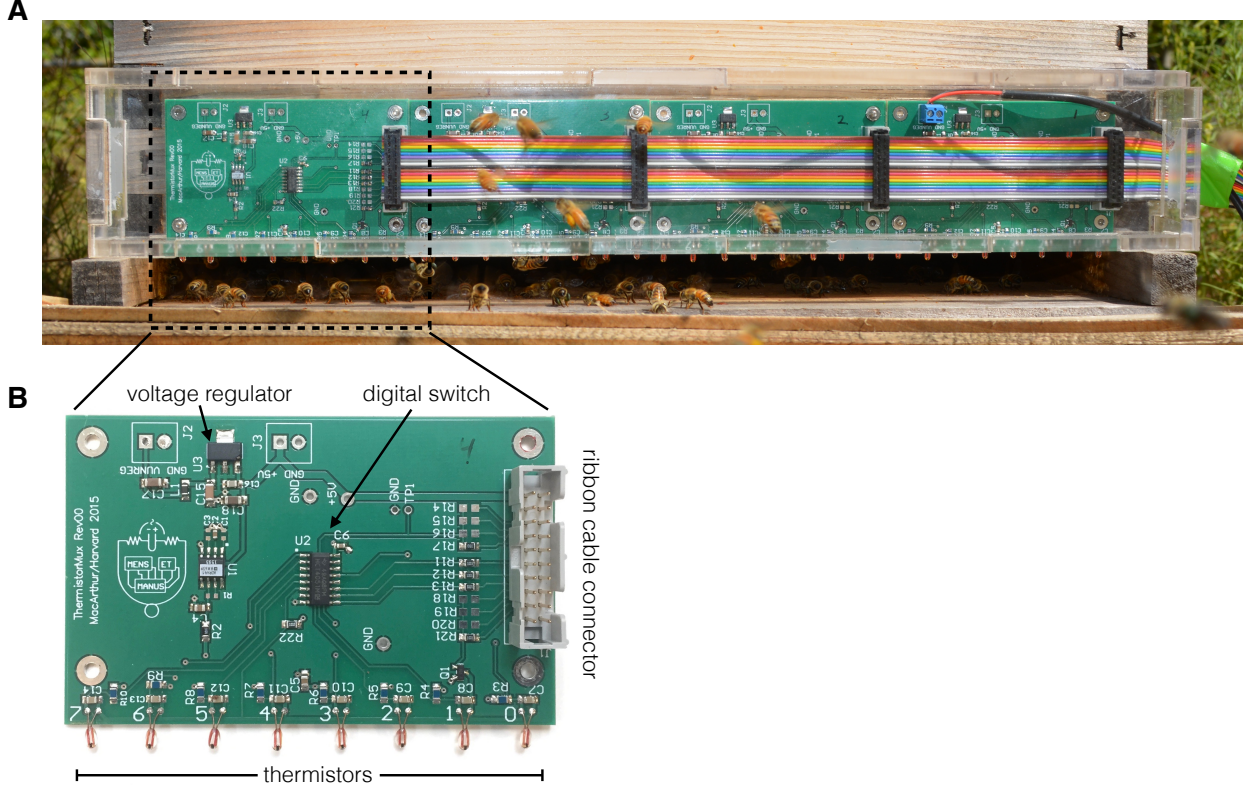


FIG. S7. Custom sensor array. A) The ThermistorMUX circuit installed at the nest entrance. B) One of four PCB modules.

TABLE S1. Dimensionless parameters and constants. Values reported here were used in simulations unless otherwise specified in the figure captions.  $L = 0.38m$ ,  $l_b = 0.02m$ ,  $v_b = 1m/s$ ,  $c = 0.05/m$ ,  $D_T = 5 \times 10^{-5}m^2/s$ ,  $D_v = 1 \times 10^{-3}m^2$ .

Parameter	Description	Value
$L/l_b$	scaled entrance length	19
$D_v/l_b^2$	scaled fluid friction	2.5
$D_T/v_b l_b$	scaled thermal diffusivity	$2.5 \times 10^{-3}$
$cl_b$	scaled fanning length	$1 \times 10^{-3}$
$m$	behavioral switch response	$0.1/^\circ C$
$\alpha$	scaled boundary conductivity	0.25

wires so that the bead of the thermistor was isolated from the circuit board and suspended in the airflow generated by the bees. The thermistors were occasionally contacted by the wings of fanning bees but they were typically not directly touching the bodies of the bees (see Fig. S8A and SI Movie 2). A Logitech c920 web cam was mounted approximately 3 ft above the nest entrance pointing down such that an orthogonal view of the "porch" was

visible. Four-second videos of fanning activity were collected every 5 minutes from 9/16/15 to 9/24/15. Temperature measurements from each of the 32 thermistors was acquired every 5 seconds over this period. An additional Parallax SHT11 digital temperature sensor was placed nearby in the shade in order to measure the ambient temperature. This protocol was repeated for two additional hives from 7/7/2016 to 7/19/2016 (Fig. S8 for complete dataset). The position of all fanning bees visible on the outside of the nest entrance during the videos taken during daylight hours were digitized by mouse click using a custom MATLAB program (See SI Movie 3). Fanning activity also occurs just inside the entrance of the hive, however these bees were not visible in our videos and are not represented in our data. We assume that analyzing the position and number of fanning bees visible in the videos is sufficient to capture the phenomena that we are interested in.

The sensor array used in this study was designed by Jim MacArthur to continuously measure air temperature at the nest entrance with high spatial and temporal resolution. The sensor array consists of four PCB modules bearing 8 thermistors each (Fig. S7). The circuit board is covered with an acrylic case. During data collection an opaque covering was used to prevent radiative heating from the sun. The thermistors were suspended in the flow stream in order to acquire an accurate air temperature without directly contacting the bees (See SI Movie 3). Each PCB module has a voltage regulator to ensure a consistent reference voltage. A digital switch allows a single digital signal to switch between each of the 8 thermistors which are read through a common analog pin. When a given thermistor is not being read, it is not receiving current, preventing self-heating. Each of modules has a ribbon cable connector allowing them to interface with the Arduino. The Arduino was programed using the Arduino IDE to select and read each thermistor in sequence. Data was transfered to a MATLAB program using a USB-Serial connection. Schematics, drawings, and code required to reproduce this setup are available on GITHUB ([ENTER STABLE LINK HERE](#)).

## **H. In large colonies $\text{CO}_2$ and temperature at the nest entrance are coupled in space but are decoupled in time**

Heat is thought to be the primary cue that induces the fanning response in honeybees. However, Seeley (1974) observed that a small colony (approximately 10,000 bees) experi-

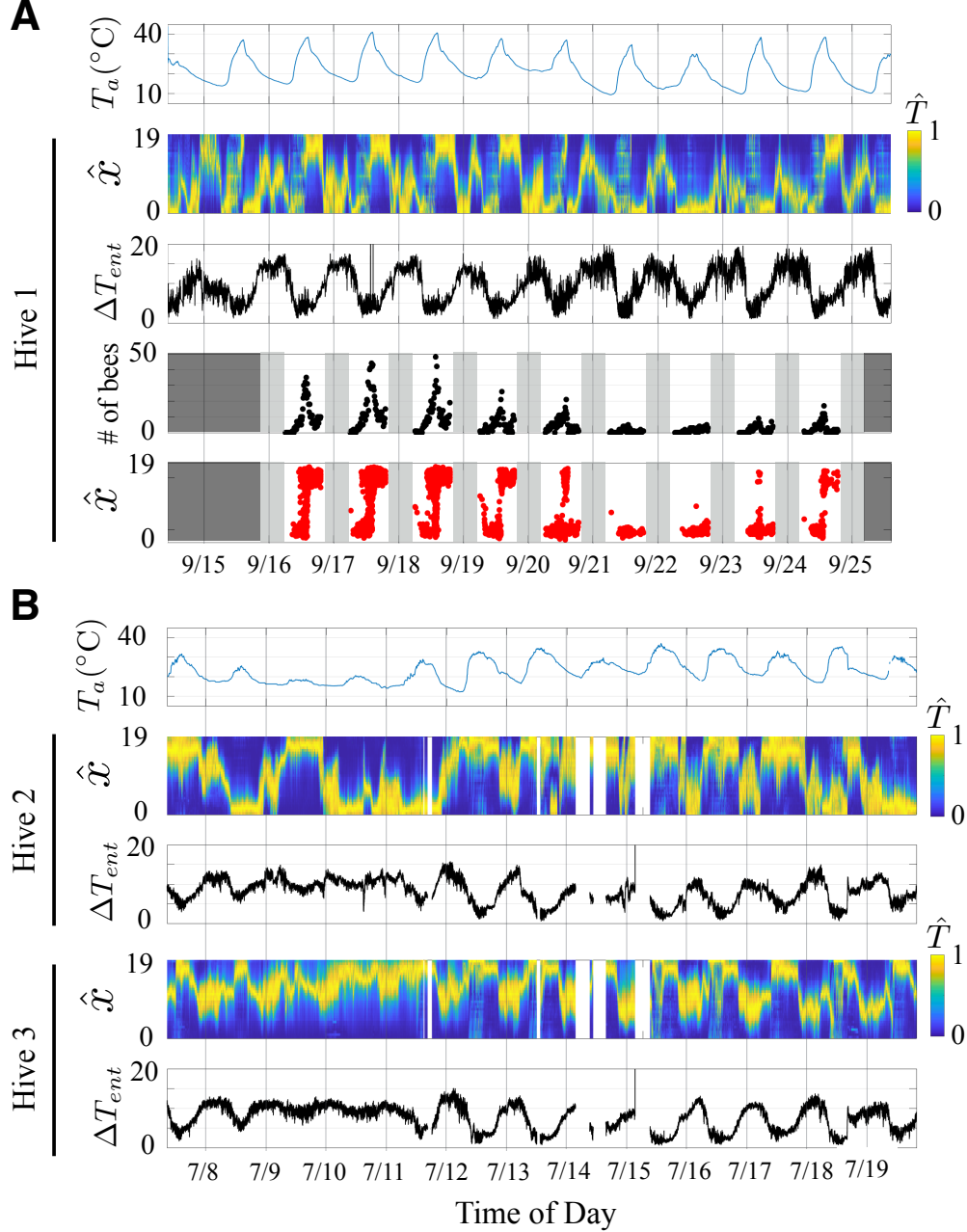


FIG. S8. Complete dataset of fanning behavior at nest entrance of three colonies in response to ambient temperature oscillations. A1) Ambient temperature,  $T_a$ , oscillations measured in the apiary from 9/14/2015 to 9/25/2015. A2) Normalized entrance temperature,  $\hat{T} \in [0, 1]$ , as measured by 32 thermistors distributed across the nest entrance. A3) The differential,  $\Delta T_{ent}$ , between the maximal (outflow) and minimal (inflow) temperature readings measured at the nest entrance at a given time. A4) The number of fanners visible at the nest entrance over time. Dark gray regions indicate times when video data was not available. Light gray regions indicate times when it was too dark to collect accurate data. A5) The position of fanning bees along the nest entrance. B1) Ambient temperature,  $T_a$ , oscillations measured in the apiary from 7/7/2016 to 7/19/2016. B2-5) Entrance temperature data for Hive 2 and Hive 3.

enced dramatic spikes in CO<sub>2</sub> concentrations which were abated by a proportional fanning response by the colony<sup>3</sup>. Over a 52 hours of CO<sub>2</sub> measurements from the brood nest of a small (10,000 bees) and large colony (35,000 bees), Seeley reported that the large colony had a lower mean CO<sub>2</sub> concentration (0.44%) than did the small colony (0.78%). In addition, the larger colony showed much less variation in CO<sub>2</sub> concentration (0.16%) than did the small colony (0.34%). Seeley suggested that this better homeostasis in CO<sub>2</sub> concentration in the large colony was likely due to near continuous thermoregulatory ventilation rather than fanning in response to CO<sub>2</sub>.

In our model, we assumed that the fanning response at the nest entrance would primarily track the local air temperature given because we were using large, mature colonies. We tested this assumption by measuring both CO<sub>2</sub> and temperature at the nest entrance of Hive 3. Because CO<sub>2</sub> sensors are larger and much more expensive than thermistors, we were not able to make a high resolution sensor array as we did for the temperature measurements. Instead, we partitioned the nest entrance into two discrete regions by placing a 15cm wooden partition in the center of the nest entrance to block airflow in this region (Fig. S9A). This allowed use to study the spatial dynamics of the fanning group while using only two CO<sub>2</sub> sensors. The bees established an outflow region on the left of the partition allowing air to passively move into the hive on the right side. This segregation of inflow and outflow emerged from the behavior of the bees and the physical constraints imposed by the partition (Fig. S9B). This configuration persisted for the three day period over which data was collected.

As expected, temperature and CO<sub>2</sub> were coupled in space—outflowing air was enriched in both CO<sub>2</sub> and heat relative to inflowing air (Fig. S9C). However, the temperature and CO<sub>2</sub> concentration of outflow were decoupled in time. The temperature of outflowing air tracked the ambient temperature. During the heat of the day when thermoregulatory ventilation was peak, CO<sub>2</sub> was at a minimum. When thermoregulatory fanning decreased during the the night, CO<sub>2</sub> was maximal. There are two possible explanations for this: 1) the number and density of bees in the nest at night is higher during the night resulting in higher CO<sub>2</sub> production, and 2) as the thermoregulatory fanning response decreases at night, CO<sub>2</sub> is evacuated at a lower rate. It seems likely that both mechanisms contribute. We also noticed an interesting dip in the CO<sub>2</sub> concentration at around 6am which was reproducible across days that we cannot yet explain.

These measurements bolster our assumption that temperature is the dominant cue in-

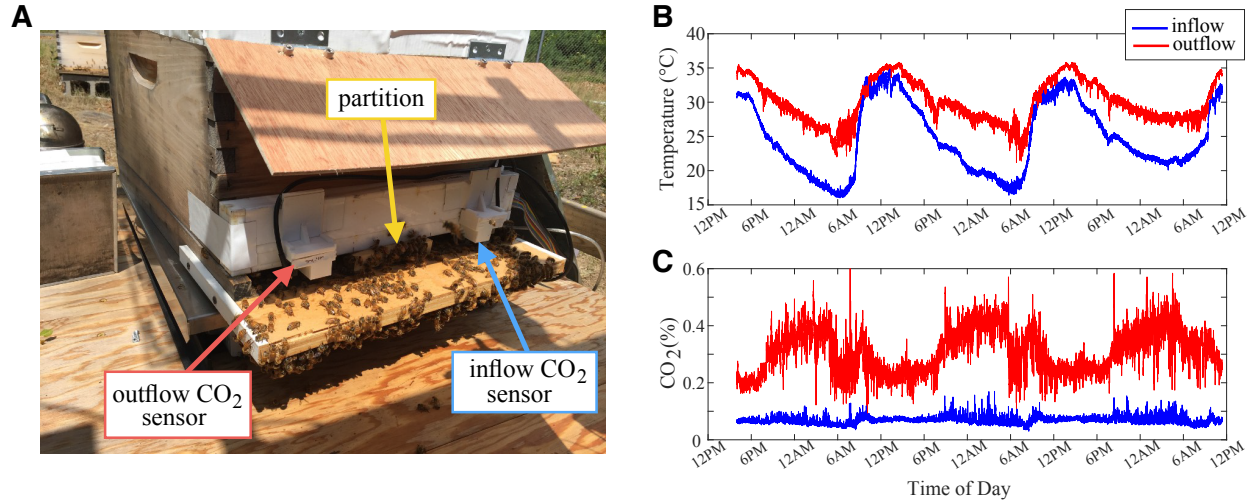


FIG. S9. A) Setup for acquiring CO<sub>2</sub> concentration data. B) Temperature of outflowing air was consistently higher than inflowing air, but varied with the ambient temperature. C) Similarly, CO<sub>2</sub> was higher in outflow than in inflow. However, CO<sub>2</sub> was decoupled from temperature, reaching a minimum during the heat of the day and a maximum at night.

ducing the fanning response in large, mature colonies. A probability function for the CO<sub>2</sub>-induced fanning response could be added to our model once it is resolved by future experimental work, but it is unlikely to qualitatively change the dynamics of the model because CO<sub>2</sub> and temperature are spatially coupled at the nest entrance.

## REFERENCES

- <sup>1</sup>J. C Jones, M. R Myerscough, S. Graham, and B. P Oldroyd. Honey Bee Nest Thermoregulation: Diversity Promotes Stability. *Science*, 305(5682):402–404, 2004.
- <sup>2</sup>C. N Cook and M D Breed. Social context influences the initiation and threshold of thermoregulatory behaviour in honeybees. *Animal Behaviour*, 86(2):323–329, 2013.
- <sup>3</sup>T. D Seeley. Atmospheric carbon dioxide regulation in honey-bee (*Apis mellifera*) colonies. *Journal of insect physiology*, 20(11):2301–2305, 1974.
- <sup>4</sup>F. Kronenberg and H C. Heller. Colonial thermoregulation in honey bees (*Apis mellifera*). *Journal of Comparative Physiology B*, 148(1):65–76, 1982.